Proceedings, XXX International Association of Hydraulic Research Congress
Thessaloniki, Greece, August 24-29, 2003

PHYSICAL AND NUMERICAL MODELING OF DELTAIC SEDIMENTATION IN LAKES AND RESERVOIRS

SVETLANA KOSTIC[1] and GARY PARKER[2]
St. Anthony Falls Laboratory, Department of Civil Engineering, University of Minnesota,
Mississippi River at 3rd Ave. SE, Minneapolis MN 55414, USA
[1]kost0067@tc.umn.edu ; [2]parke002@tc.umn.edu

ABSTRACT

Deltas form where rivers meet standing bodies of water such as lakes and reservoirs. A delta is composed of a coarse-grained fluvially-deposited topset, a coarse-grained prograding foreset deposited by grain avalanching and a fine-grained bottomset deposited from a surface sediment plume or a plunging turbidity current. Here the case of a 1D delta in a body of fresh water with a bottomset emplaced by a plunging turbidity current is considered. The authors have previously developed a moving-boundary numerical model pertaining to such deltas. In that model the coarse-grained material is characterized with a single sand size and the fine-grained material is characterized with a single mud (silt-clay) size that drives the plunging turbidity current. Here the analysis is extended to the case for which the turbidity current is driven by two agents: mud and dissolved salt. Salt serves as a surrogate for a mud so fine that its fall velocity can be neglected. The results of the numerical model are tested against an experiment.

Keywords: deltas, sediment, rivers, turbidity current, numerical model

INTRODUCTION

Fluvial fans are cone-shaped zones of sedimentation downstream of an upland sediment source. They may be completely terrestrial, or may have a distal portion ending in standing water. An illustrative example of the former type is the fan of the Kosi River, India, which emanates from the Himalaya Mountains (Fig. 1). Fans of the latter type are called fan-deltas, examples of which are shown in Fig. 2 (natural) and Fig. 3 (modified by human interference).

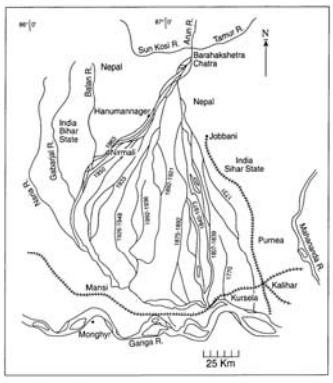

Figure 1. History of channel change on the Kosi Fan, India (Gole and Chitale, 1966).

Figure 2. Fan-delta in the Yukon, Canada.

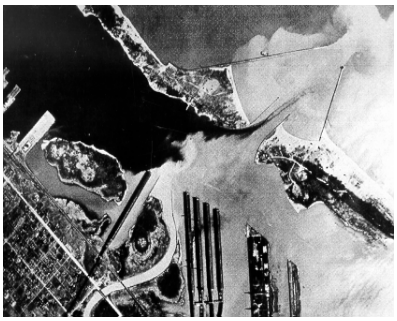

Figure 3. Sediment from the Nemadji River, USA enters Lake Superior at Superior Harbor.

The most common morphology associated with fan-deltas is that of sand-bed streams. These usually carry significantly more mud as wash load than they do sand as bed-material load. The typical structure of a deltaic deposit in a lake or reservoir is illustrated in Fig. 4 (e.g.

Vanoni 1975). The sand is emplaced fluvially on the topset and by avalanching on the foreset. The mud-laden water during floods may form a surface plume, from which the sediment rains down to emplace the bottomset deposit. In other cases, however, this water plunges over the steep delta face and continues to flow downslope into deep water as a muddy turbidity current, which then emplaces the bottomset deposit. This latter case is considered here. The foreset sand tends to prograde over the bottomset mud in time as all three regions interact with each other.

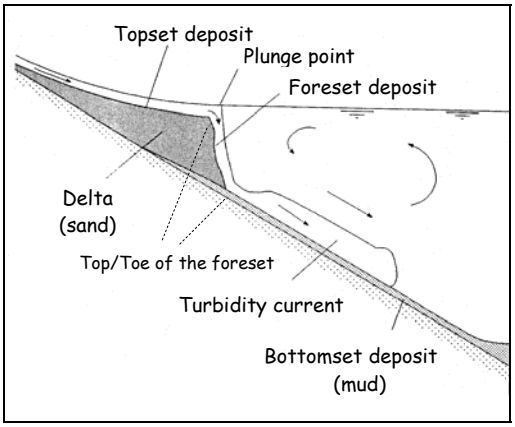

Figure 4. Typical structure of a deltaic deposit in a lake or reservoir

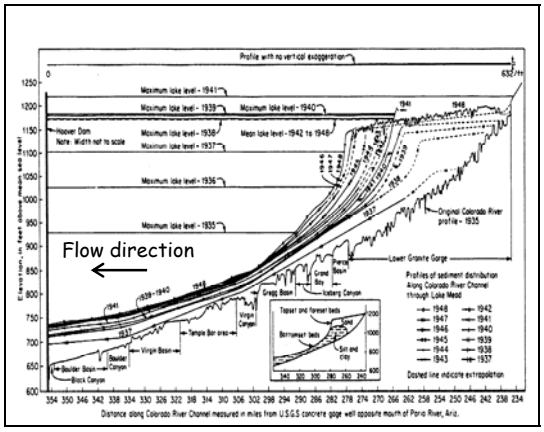

Figure 5. Deposition pattern along the Colorado River through Lake Mead, 1935-1948.

The Colorado River, for example, rapidly constructed a large delta at the head of Lake Mead after the closing of Hoover Dam. Fig. 5 (Grover & Howard 1937) documents the development of a sandy topset and foreset, and muddy bottomset, from 1935 to 1948, after which time the construction of Glen Canyon Dam upstream cut off most of the sediment supply. Of particular interest is the interface between the foreset sand and the bottomset mud, which behaves as a moving boundary.

MOTIVATION

Deltaic sedimentation can seriously limit the performance of a river-fed reservoir and cause significant morphological changes in the river channel. Some of the repercussions imposed by sedimentation processes in reservoirs and lakes are: loss of available storage, increased risk of flooding, silting up of harbors in the upper river reach, blockage of intake structures, sediment entrainment at power plant intakes, and problems with navigation.

The numerical model reported here was motivated by the delta of the Nemadji River, USA at Superior Harbor, where it flows into Lake Superior (Fig. 3). The mean annual loading of the stream at Superior Harbor is about 131,000 t/yr, 89 % of which is mud and the rest being sand. Kostic & Parker (in press (a), in press (b)) developed a 1D moving-boundary numerical to capture the co-evolution of the topset, foreset and bottomset in such deltas. They verified their model against two experiments and applied it at field scale. That model includes one grain size to characterize the sand which deposits on the topset and foreset, and another grain size to characterize the mud which deposits on the bottomset.

Here the model is extended to include a conservative phase in addition to the mud phase. The conservative phase is realized experimentally with the addition of dissolved salt to the river water. The turbidity current is then driven by the excess weight of both the mud and the

dissolved salt. The dissolved salt serves as a surrogate for a second mud phase that is too fine to settle out in the reservoir. The extended model is verified against an experiment similar to the two used to verify the earlier model.

MODEL FORMULATION

The model consists of two coupled submodels: (1) a fluvial delta model that describes the deposition of sand on the river bed and its avalanching down the delta face into deeper water; (2) a turbidity current model that predicts the evolution of the bed of a lake or reservoir as a result of the deposition of mud from a plunging turbidity current. The turbidity current is driven by a combination of two mud phases, one coarse enough to settle out with fall velocity v_m and the other so fine that its fall velocity can be neglected. In the experiment discussed below the fine phase is replaced with dissolved salt as a surrogate. With this in mind the two phases that drive the turbidity current are referred to below as "mud" and "salt" for simplicity.

Fluvial Submodel The relations governing the flow in the fluvial zone, i.e. upstream of the top of the foreset include the conservation of fluid mass, downslope momentum and bed sediment. The hydrodynamic part of the model encompasses the quasi-steady flow approximation (e.g. de Vries, 1965) since the variation of discharge in many low-slope rivers is sufficiently gradual so as to allow the assumption of steady flow in each step of hydrograph.

$$U_f h_f = q_w \tag{1}$$

$$\frac{\partial}{\partial x}\left(\frac{1}{2}U_f^2 + g h_f + g\eta_f\right) = -C_f \frac{U_f^2}{h_f} \tag{2}$$

$$\left(1-\lambda_S\right)\frac{\partial \eta_f}{\partial t} = -\frac{\partial q_S}{\partial x} \tag{3}$$

where x = streamwise distance,, t = time, g = acceleration of gravity, q_w = water discharge per unit width, λ_S = porosity of sand deposit, q_S = volume transport rate of sand per unit width (total bed material load), and C_f = bed friction factor. The dependent variables are the depth of fluvial flow h_f, the river velocity U_f and the elevation of the river bed η_f.

In most sand-bed rivers near a delta the flow is subcritical in the Froude sense, so that (1) and (2) reduce to the standard backwater formulation. However, during the course of three experiments designed to verify the numerical model at hand (Kostic & Parker, in press (b)), the flow was either supercritical or near-supercritical, with the Froude number slightly below unity. In such a case (2) can be approximated in terms of quasi-uniform normal flow

$$C_f U_f^2 = -g h_f \frac{\partial \eta_f}{\partial x} \tag{2a}$$

In order to close the above governing equations the friction coefficient C_f is assumed to be constant, and the sand transport rate q_S is evaluated form the Engelund-Hansen relation for total bed material load (Engelund & Hansen, 1972).

Initial and boundary conditions for the fluvial model are discussed in detail in Kostic & Parker (in press (a)). They are briefly summarized herein. At time t = 0, the elevation of the topset bed for every grid point within the fluvial domain is determined from a specified initial slope S_{f0} of the fluvial bed. Three boundary conditions on the fluvial domain are required, one for the fluvial inflow boundary and two for the outflow boundary. These are specified as follows:

$$q_S\big|_{x=0} = q_{S0}\ ,\quad q_S\big|_{x=f} = \left(1-\lambda_S\right)\dot{f}\left(\eta_f\big|_{x=f} - \eta\big|_{x=l}\right) \tag{4,5}$$

$$h_f\Big|_{x=f} = Z_l - \eta_f\Big|_{x=f} - d\,\Delta h\Big|_{x=f}, \quad \Delta h = 0.5\,h_f\Big|_{x=f}\left(-3+\sqrt{1+8Fr^2\Big|_{x=f}}\right) \tag{6}$$

where q_{S0} is the volume sand feed rate per unit width, $\eta_f\Big|_{x=f}$ and $\eta\Big|_{x=l}$ denote the elevation of the top (where $x = f$) and toe (where $x = l$) of the foreset deposit respectively, and $\dot{f}$ is the rate of delta face progradation. Z_l denotes the water surface elevation of the lake or reservoir (taken to be constant in time in the present analysis), $Fr\Big|_{x=f}$ the Froude number at the top of the foreset, and $\Delta h\Big|_{x=f}$ = the height of the hydraulic jump formed when supercritical flow impinges upon an infinite body of standing water. Finally, d is a coefficient defined such that $d = 0$ for subcritical river flow (the usual case in the field) and $d = 1$ for supercritical flow (a common occurrence in the experiments).

Equation (5) represents the simplest implementation of a delta-front "shock condition" which is derived in Swenson et al. (2000) and Kostic & Parker (in press (a)). This condition imposes a balance between the sand delivered to the top of the foreset deposit and the rate of delta face progradation.

Turbidity current submodel The layer-averaged equations of a dense bottom underflow flowing into an unstratified, fresh body of water are considered below (Kostic & Parker, in press (a));

$$\frac{\partial h}{\partial t} + \frac{\partial Uh}{\partial x} = e_w U \tag{7}$$

$$\frac{\partial Uh}{\partial t} + \frac{\partial U^2 h}{\partial x} = -\frac{1}{2} g \frac{\partial \phi h^2}{\partial x} - gh\phi \frac{\partial \eta}{\partial x} - c_D U^2 \tag{8}$$

$$\frac{\partial Ch}{\partial t} + \frac{\partial CUh}{\partial x} = -r_o v_m C \tag{9}$$

$$\frac{\partial Sh}{\partial t} + \frac{\partial SUh}{\partial x} = 0 \tag{10}$$

$$(1-\lambda)\frac{\partial \eta}{\partial t} = r_o v_m C \tag{11}$$

In the above relations h = underflow thickness, U = layer-averaged underflow velocity, ϕ = layer-averaged excess fractional density of the underflow, C = layer-averaged volume concentration of mud and S = layer-averaged concentration of dissolved salt within the underflow. In addition, e_w = entrainment coefficient of ambient water into the underflow, c_D = bottom friction coefficient of the underflow, λ = porosity of the bottomset deposit, v_m = fall velocity of the mud, and r_o = an order-one multiplicative constant. The parameters ϕ, C and S are related as follows;

$$\phi = RC + \beta S \tag{12}$$

where R = submerged specific gravity of the mud and β = coefficient based on a linearized relation between salt concentration S and fraction excess density.

In order to close (7 - 12) c_D and r_o are assumed to be prescribed constants and e_w is taken to be a prescribed function of the flow Richardson number Ri, given as

$$Ri = g\phi h / U^2 \tag{13}$$

The mud fall velocity v_m is calculated from the relation of Dietrich (1982).

Initial and boundary conditions for the turbidity current model are discussed in detail in Kostic & Parker (in press (a)). At $t = 0$ the dependent primitive variables h, U, C and S at all nodal points are set equal to their values h_o, U_o, C_o and S_o immediately after the river inflow plunges to form an underflow. The plunging formulation incorporated in the turbidity current model is described in Kostic & Parker (in press (a)). The initial elevation of the bottomset bed for every grid point is determined from a prescribed initial slope S_o of the bed of the lake or reservoir. Because of the hyperbolic nature of governing equations, the number and location of physical boundary conditions correspond to the number and location of characteristics that propagate into the flow domain (Kostic & Parker, in press (a)). For an underflow that is supercritical in the Richardson sense, there are three physical inflow boundary conditions, and two outflow boundary conditions. These are formulated as follows.

The inflow boundary conditions take the form

$$h\left(x=l,t\right)=h_o\ ,\ U\left(x=l,t\right)=U_o\ ,\ \vartheta\left(x=l,t\right)=\vartheta_o \tag{14-16}$$

where ϑ is the new primitive variable, defined as

$$\vartheta=\varphi_{SO}C+(1-\varphi_{SO})S \tag{17}$$

The buoyancy ratio $\varphi_{So}=RC_o/(RC_o+\beta S_o)$ immediately after the plunge point represents the fraction of the buoyancy force that derives from the presence of suspended sediment (as opposed to dissolved salt).

The outflow boundary conditions take the form

$$U\left(x=s,t\right)=\frac{ds}{dt}\ ,\ \eta\left(x=s,t\right)=\eta_o\left(s\right) \tag{18,19}$$

where η_o is an antecedent bed elevation as yet unmodified by the turbidity current, and s denotes the position of the turbidity current head. The remaining variables are obtained from the flow domain by means of first-order extrapolation.

NUMERICAL SCHEME AND LINKING OF SUBMODELS

The turbidity current model is handled by the explicit ULTIMATE QUICKEST method (Leonard 1979 & 1991), which is third order in both time and space. The scheme provides a robust, mass-conservative formulation that is capable of dealing with highly advective transport and complex boundary conditions. The sediment part of the fluvial model is handled by the explicit QUICKEST method, while the hydrodynamic part is solved with a second-order Runge-Kutta scheme in the case of subcritical flow. For supercritical flow the sediment part is solved by means of the explicit QUICKEST method for all computational points except the one farthest downstream, where the slope is determined by a Newton-Raphson iterative procedure.

The fluvial model is linked to the turbidity current model via the physical outflow boundary condition (5) for the fluvial model and a numerical inflow boundary condition for the underflow model. The latter condition imposes continuity of bed elevation at the foreset-bottomset break, which for constant foreset slope S_a takes the form

$$\left.\frac{\partial\eta_f}{\partial t}\right|_{x=f}=\left.\frac{\partial\eta}{\partial t}\right|_{x=l}+\dot{l}\left(S\big|_{x=l}+Sa\right)-\dot{f}\left(S_f\big|_{x=f}+S_a\right) \tag{20}$$

where $S\big|_{x=l}$ denotes the bottomset slope at the toe of the delta face, $S_f\big|_{x=f}$ is the topset slope at the top of the delta face, and $\dot{l}$ is the speed of progradation of foreset-bottomset break.

MODEL VERIFICATION

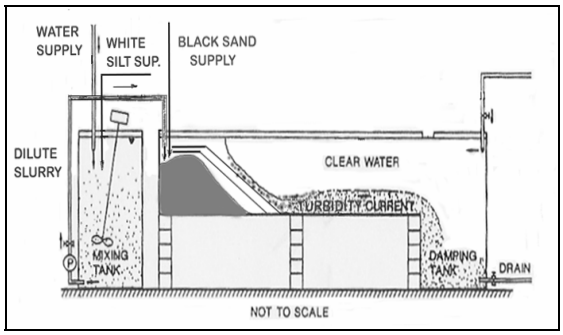

Figure 6. Experimental set-up.

The numerical model outlined above was tested against two experiments (Experiments 1 and 2) on progradational sand-mud deltas carried out at St. Anthony Falls Laboratory, University of Minnesota and reported in Kostic and Parker (in press (b)). Both experiments were performed with a black sand and white mud, without the addition of dissolved salt in the inflowing water. The experimental facility, shown in Figure 6 incorporates a flume that was specially modified to allow the modeling of continuous turbidity currents extending for up to one hour (Garcia 1994). Details on experimental set-up and procedure can be found in Kostic & Parker (in press (b))

Two images documenting these experiments are presented in Figs. 7 and 8. Fig. 7 illustrates the sand-mud delta just a few seconds before the completion of Experiment 2. Coal has been placed into the flow to allow for visualization of the turbidity current. Topset, foreset and bottomset deposits are clearly defined. The turbidity current typically plunged one-third of

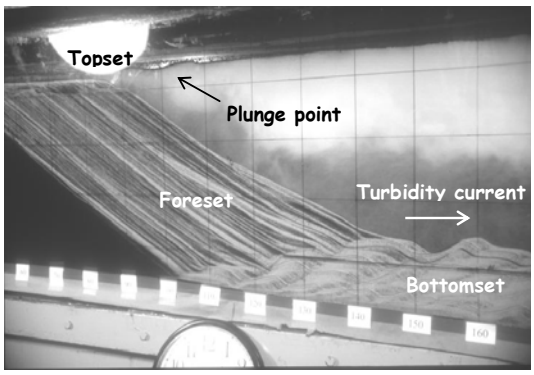

Figure 7. Resulting fan-delta right before the end of Experiment 2.

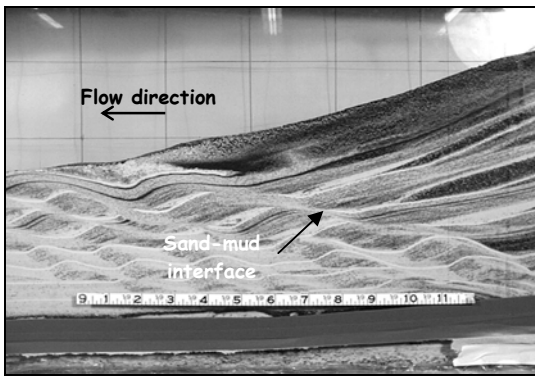

Figure 8. Expanded view of moving boundary in Experiment 1.

the way down the foreset slope. The passage of six turbidity currents over the sandy foreset reduced the slope of the foreset deposit from 35^o to an average of 29.2^o. An expanded view of the interface between the foreset and bottomset at the end of Experiment 1 is shown in Fig. 8. The numerical model proved able to reproduce the results of these two experiments with a minimum of tuning, as outlined in Kostic and Parker (in press (a), in press (b)).

An additional experiment, Experiment 3 was conducted with the presence of dissolved salt in the inflowing muddy water in order to a) increase the strength of the turbidity current and c) study the effect of a conservative component in the turbidity current, i.e. a component that is not lost due to settling. The black sand and white mud were the same as those used in Kostic and Parker (in press (b)). The channel width was 0.305 m. The inflow rate of water was 2 l/s. In the first part of the experiment only black sand was fed into the channel at a rate of 32.6 g/s, allowing a Gilbert delta to build out, and forming the profile T0 in Fig. 9. In the second part of the experiment white mud (silica flour) was mixed into the water and fed into the channel at a rate of 103.3 g/s, without halting the supply of black sand. Four runs of about 14

minutes each were continued in this way, making the deposit profiles denoted T1 – T4 in Fig.9.

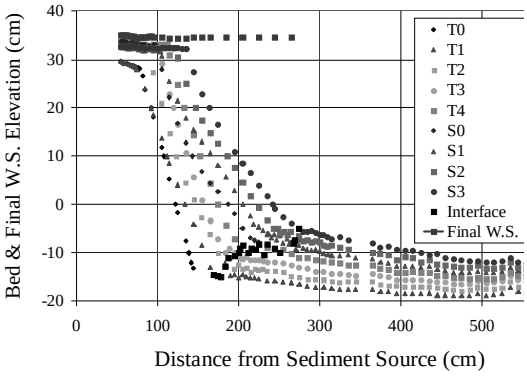

Figure 9. Measured bed profiles for Exp. 3.

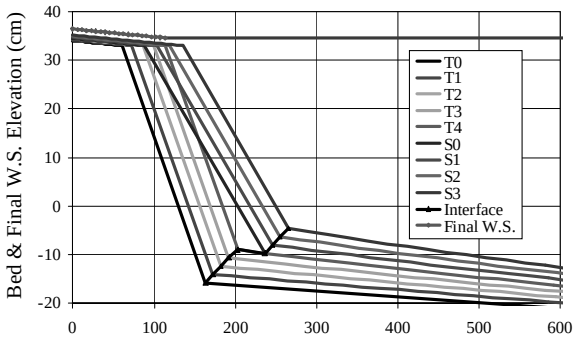

Figure 10. Numerical simulation of Exp. 3.

In Fig. 9 the profile S0 describes the new morphology due to a slide event caused by a slight variation in water surface elevation after the cessation of run T4. Profiles S1 - S3 correspond to the resulting deposits at the end of three consecutive 14-minute runs for which the underflows were driven by the combination of mud and dissolved salt. The concentration of dissolved salt was 41.19 ppt, and the excess density of the inflow water about 0.0644 (nearly twice as high as for the case with mud but no salt), resulting in a notably increased strength of the muddy underflow. The experiment confirmed an earlier result of Kostic et al. (2002), according to which a muddy turbidity current overriding a sandy foreset can substantially reduce the foreset angle. The average slope of the foreset deposit for the run T0 with only black sand was found to be 35.5°; in the runs T1 – T4 with white mud but no salt the angle was reduced to d to be 25.48°. With the addition of salt in runs S1 – S3 the foreset angle was further reduced to 16.10°.

The moving-boundary numerical model presented above was used to simulate Experiment 3. The conditions of the simulation were very similar to those outlined in Kostic and Parker (in press (b)), except that a) the effect of dissolved salt was included and b) careful attention was paid to the decline in foreset angle caused by overrun of the foreset by a) a muddy turbidity current and b) a muddy turbidity current strengthened with dissolved salt. The numerical simulation of Fig. 10 was obtained with a minimum of data fitting. Note that the initial condition for the numerical simulation of run S1 was adjusted to reflect the slide on the delta foreset observed in the experiment.

CONCLUSIONS

The numerical model presented in Kostic and Parker (in press (a), in press (b)) is the first interactive, physically-based model of deltaic sedimentation in lakes and reservoirs, capable of capturing the essence of the topset, foreset and bottomset deposition in lakes and reservoirs, and reproducing the evolution of the sand-mud interface in deltas. Here the model is extended to include a conservative component to the turbidity current. The model was tested against data for an experiment, Experiment 3, in which the conservative component was dissolved salt, which acted to intensify the turbidity current. Good agreement with data was obtained with a minimum of tuning.

An interesting feature of Experiment 3 was a marked reduction in the foreset angle with increasing strength of the turbidity current overriding it. In the absence of an overriding turbidity current, the foreset prograded at the angle of repose of 35.5°. The overriding turbidity current reduced the foreset angle to 25.48°. Further addition of dissolved salt to the turbidity current reduced the angle to 16.10°. These observations are in line with the theoretical formulation of Kostic et al. (2002), who indicate the possibility of a reduction in foreset angle to as low as 1° in the field by the same mechanism.

ACKNOWLEDGEMENTS

This research was funded by Minnesota Sea Grant and the National Center for Earth-surface Dynamics; the Center is funded by the National Science Foundation. This paper represents a contribution of the National Center for Earth-Surface Dynamics.

REFERENCES

DE VRIES, M. (1965). Consideration about non-steady bed-load transport in open channels. *Proceedings*, IAHR 11th Congress, 3.8.1-3.8.8.

DIETRICH, E. W. (1982). Settling velocity of natural particles. *Water Resources Research*, 18(6), 1626-1982.

ENGELUND, F. & HANSEN, E. (1972). *A monograph on sediment transport*. Technisk Forlag, Copenhagen, Denmark.

GARCIA, M. (1994). Depositional turbidity currents laden with poorly sorted sediment: *Journal of Hydraulic Engineering*, 120(11), 1240-1263.

GROVER, N. C. & HOWARD, C. L. (1937). The passage of turbid water through Lake Mead: *Transactions* American Society of Civil Engineers, 103, 720-732.

GOLE, C. V. & CHITALE, S. V. (1966). Inland delta building activity of the Kosi River. *Journal of Hydraulic Engineering*, 92(2), 111-126.

KOSTIC, S. & PARKER, G. (in press (a)). Progradational sand-mud deltas in lakes and reservoirs: Part 1. Theory and numerical modeling. *Journal of Hydraulic Research*.

KOSTIC, S. & PARKER, G. (in press (b)). Progradational sand-mud deltas in lakes and reservoirs: Part 2. Experiment and numerical simulation. *Journal of Hydraulic Research*.

KOSTIC, S., PARKER, G. & MARR, J. (2002) Role of turbidity currents in setting the foreset slope of clinoforms prograding into standing fresh water, *Journal of Sedimentary Research*, 72(3), 353-362.

LEONARD, B.P. (1979). A stable and accurate convection modeling procedure based on quadratic upstream interpolation. *Comp. Methods in Applied Mechanics and Engineering*, 19, 59-98.

LEONARD, B.P. (1991). The ULTIMATE conservative difference scheme applied to unsteady one-dimensional advection. *Comp. Methods in Applied Mechanics and Engineering*, 88, 17-77.

SWENSON, J. B., VOLLER, V. R., PAOLA, C., PARKER, G. & MARR, J. (2000). Fluvio-deltaic sedimentation: A generalized Stefan problem. *European Journal of Applied Math.*, 11, 433-452.

VANONI, V. A. (1975). *Sedimentation Engineering*. American Society of Civil Engineers, New York N.Y., 745 p